Temporal segmentation of the stochastic oscillator neural network

Seung Kee Han,[1] Won Sup Kim,[1] and Hyungtae Kook[2]
[1]*Department of Physics, Chungbuk National University, Cheongju, Chungbuk 361-763, Korea*
[2]*Department of Physics, Kyungwon University, Sungnam, Kyunggi 461-701, Korea*
(Received 24 December 1997; revised manuscript received 27 April 1998)

We propose a stochastic oscillator neural network model of the Hopfield-type memory for pattern segmentation tasks exploiting temporal dynamics of stochastic nonlinear oscillators. The nonlinear oscillators in the model are driven by subthreshold periodic force and noise. For an input pattern which is an overlapped superposition of several stored patterns, it is shown that the proposed model network is capable of segmenting out each pattern one after another as synchronous firings of a group of neurons. A systematic study of the dependence on the model parameters shows that the temporal segmentation attains its optimal performance at an intermediate noise intensity, which is reminiscent of the stochastic resonance observed in the coupled oscillator networks. It is also shown that the inhibitory coupling between oscillator groups representing different patterns plays an important role in that it enhances both the firing rate and the intergroup desynchrony that are essential requirements for the optimal performance of the temporal segmentation. [S1063-651X(98)06808-1]

PACS number(s): 84.35.+i, 02.50.Ey, 05.40.+j, 82.40.Bj

I. INTRODUCTION

Recently, electrophysiological experiments on the visual cortex of a cat have revealed the presence of oscillatory rhythms in the measurement of the local field potential upon the presentation of moving visual stimuli [1,2]. The observation of a 40–60-Hz synchronous oscillation among neurons that are widely separated over the visual cortex has supported the idea that temporal correlation among the neurons is the working mechanism for the feature binding [3,4]. The processes of perception—like the figure-background separation, the object recognition, and the separation of distinct objects—are all based on the feature binding mechanism. Recent studies on the functional role of the nervous system have concentrated on the dynamic behavior of the nervous system [4–6].

Motivated by physiological evidence of synchronous oscillations as the means of the feature binding, a new approach using the associative oscillator neural network has been proposed to resolve the so-called superposition catastrophe problem [7]. That is, when an input corresponding to a superposition of several stored patterns is presented for conventional associative neural networks whose performance is based on fixed-point dynamics [8,9], it is viewed as a new pattern that has not been stored. Therefore, the network is not able to retrieve information for the hidden component patterns. Meanwhile, in the associative oscillator network each component pattern pops out as a synchronous firing of a subgroup of neurons, and the different patterns are distinguished by the different temporal activities of the subgroups, which is the main idea of the temporal segmentation scheme. Therefore, the oscillatory network is shown to be capable of avoiding the superposition catastrophe problem. Since then, various models using the oscillatory neural networks have been attempted for the temporal segmentation tasks.

In Refs. [10,11], the dynamic threshold in the Hopfield neural network was incorporated to obtain an oscillatory neural network, and in Refs. [12,13] an oscillator network was constructed using oscillator units, each of which is a feedback loop of the excitatory and inhibitory cells. These models have been shown to exhibit the capability to retrieve component patterns for a small number of the superimposed input patterns, which is achieved in a rather brief period. As considered in Ref. [14], however, the deterministic oscillator models previously employed have an inherent limitation in the capacity of the temporal segmentation. That is, as the number of the superimposed patterns increases, the network often falls into partially segmented states that correspond to occurrences of the fusion of several component patterns. The effect of noisy inputs on segmentation was also examined, and it was reported that noise in some cases can enhance the performance [15], even though it is not sufficient to remove the basic limitation.

On the other hand, it was recently observed that noise can play a supportive role, counterintuitively, in detecting weak signals. That is, when a weak periodic force is applied to a nonlinear system with a threshold, the signal-to-noise ratio shows an optimal peak at an intermediate level of the noise intensity. This phenomenon has been referred to as ''stochastic resonance'' in the literature [16]. Since its introduction in explaining the periodicity of the Earth's Ice Ages [17], stochastic resonance has been studied in a variety of contexts including ring lasers [18], the electronic circuit [19–21], and sensory neuronal systems [22–24]. Recently, it was also demonstrated through a psychophysical experiment that stochastic resonance can be used as a quantitative measure of the efficiency with which the visual system processes noisy information [25].

In the present work, motivated by observations of the active role of noise, we propose an oscillator neural network model of Hopfield-type memory for pattern segmentation tasks which exploit temporal dynamics of stochastic nonlinear oscillators; the stochastic oscillator neural network proposed will hereafter be abbreviated as STONN. The proposed model is different from previous oscillator network models [10–12,14] in that the nonlinear oscillators of the

network are driven by the subthreshold periodic force and noise, which leads to a segmentation mechanism different from the previous attempts. That is, the segmentation task is carried out in the STONN when each pattern is selected to fall into the firing state one after another by noise, while the other patterns not selected at a moment remain in the resting state. In Refs. [10–12,14], all pattern activities maintain oscillatory states with phase shifts among them, and such a train of the staggered oscillations is regarded as the desired segmentation. We expect that the proposed model, incorporating an active role of noise, may provide an alternative approach of constructing associative memories for the temporal segmentation tasks.

In the following it is shown that the proposed model network has the capability of temporal segmentation. A systematic study of the dependence of the performance on the model parameters shows that the performance of the proposed model attains its optimal value at an intermediate level of the noise intensity, which is reminiscent of the stochastic resonance observed in the coupled oscillator networks [26]. This paper is organized as follows. In Sec. II, we introduce a stochastic one-dimensional nonlinear oscillator as a simplified neuron model. In Sec. III, the effects of noise as well as coupling between oscillations are examined in detail with the simplest example of two coupled oscillators. It is shown that the inhibitory coupling between oscillators plays a distinctive role which turns out to be very essential for the optimal performance of the proposed network model. The STONN is constructed, using the Hopfield-type memory, in Sec. IV. The performance of the network for the memory retrieval is also examined. In Sec. V, the performance of the proposed network for the temporal segmentation is examined for various ranges of the noise intensity as well as the coupling strength, and explanations for such behavior of the network are attempted based on the observations from the two coupled oscillators. Finally, in Sec. VI we make conclusions with discussion.

II. STOCHASTIC NONLINEAR OSCILLATOR

In the presence of a sufficiently strong sinusoidal stimulus, a neuron can be excited from the stationary resting state to the oscillatory firing state. In this paper such an activation of a neuron from the resting state to the firing state is described by a one-dimensional overdamped nonlinear oscillator, which can be regarded as a further simplified version of the more realistic models such as the Hodgkin-Huxley [27], Fitzhugh-Nagumo [28,29], or Morris-Lecar [30] neuron models. The simplification to the one-dimensional oscillator model greatly reduces the computational complexity of the coupled neural oscillators system.

Dynamics of the activation variable x representing the membrane voltage of a neuron is governed by the ordinary differential equation

$$\frac{dx}{dt} = -\frac{dU(x)}{dx} + I(t) + \sqrt{2D}\xi, \tag{1}$$

where the potential is given as $U(x) = -1/2x^2 + 1/4x^4$. As shown in Fig. 1, the potential has a threshold at $x_c = 0$, which denotes the crossover from the resting state to the firing state

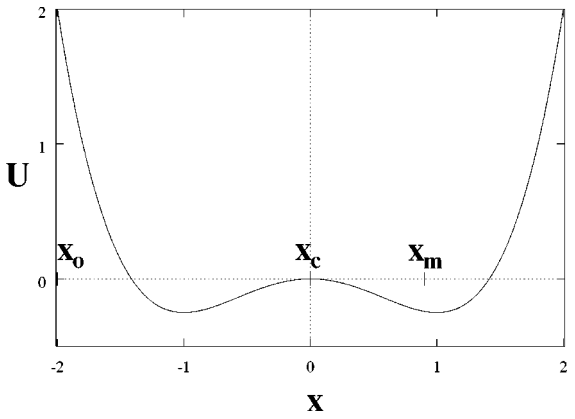

FIG. 1. Double well potential of the oscillator in Eq. (1).

of the neuron. That is, the neuron is regarded as being in the resting state when $x<0$, and in the firing state when $x>0$. For a real neuron the firing state usually lasts for only a brief period, and is followed by the deactivation process, restoring the membrane potential back to the resting state. This mechanism of deactivation is introduced in our model by holding the activation variable x for a brief time delay, and then resetting it to $x=x_0$ whenever x reaches a prescribed value x_m; x_m and x_0 indicated in the figure can be chosen arbitrarily, since their precise values do not lead to an appreciable change in the results. We set $x_m = 0.9$ and $x_0 = -2.0$ in the present work.

A periodic driving force $I(t) = I_0 \sin(\omega_0 t)$, with $\omega_0 = 0.1$, represents an input stimulus. When the strength of stimulus I_0 is larger than the threshold value $I_{\text{th}} \sim 0.42$, the model neuron exhibits sustained periodic firings. When the input stimulus is weak below the threshold value, x cannot reach the firing state and just wobbles around the resting state. In the present work, if not specified, the input stimulus is assumed to be in the subthreshold regime, $I_0 = 0.36$, so that it does not excite the neuron by itself. However, in the presence of noise, as added in the last term of Eq. (1), the model neuron can be driven to the firing regime even with the subthreshold stimuli, which is the main phenomenon exploited in the present work. D is the noise intensity, and the random white noise ξ is defined as

$$\langle \xi(t) \rangle = 0, \quad \langle \xi(t)\xi(t') \rangle = \delta_{t,t'}. \tag{2}$$

However, the firing events are only rare when the noise intensity D is rather small. The firing occurs more frequently as the level of the noise intensity becomes higher. When the noise level is too high, however, the occurrence of the firings becomes noisy; that is, most firings become incoherent with the driving force $I(t)$. Therefore, the coherent firing of the neuron is a cooperative behavior between noise and the driving force. That is, whenever the periodic driving force is at its peak value, the neuron has a chance to fire through the additional forcing provided by noise. Figure 2 shows the power spectral density $P(\omega)$ of the output signal $x(t)$, which displays δ peaks at the frequency ω_0 of the driving forcing and also at its harmonics. The stochastic resonance is manifested by the signal-to-noise ratio (SNR) of $x(t)$, which is the logarithm of the ratio of the power spectral density $P(\omega_0)$ to the background noise intensity [18]. The inset of

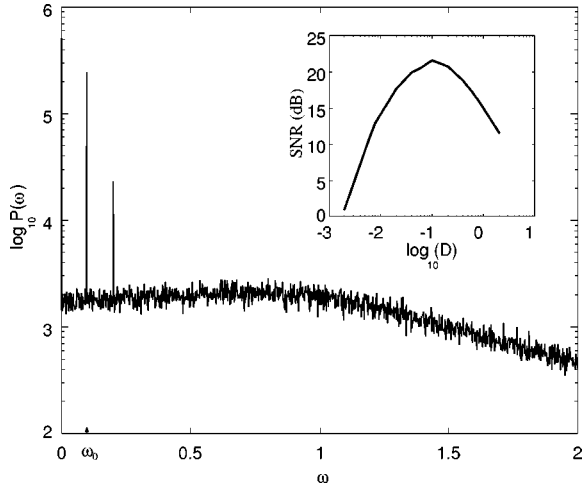

FIG. 2. Power spectral density $P(\omega)$ for $x(t)$ at $D=0.1$. The inset shows the SNR as a function of D.

the figure shows the SNR as a function of the noise intensity D. As shown in the figure, the SNR peak occurs at the noise intensity $D=D_0\sim 0.1$. The appearance of the SNR peak at an intermediate noise intensity is a universal behavior of nonlinear systems, with the threshold dynamics like the one of the present neuron model [16,17,19–24].

III. TWO COUPLED OSCILLATORS

Before examining the more complex behavior of the oscillator networks, let us first consider the simplest case of two coupled stochastic oscillators. The system is described by the following coupled differential equations:

$$\frac{dx_1}{dt}=-\frac{dU(x_1)}{dx_1}+I_1(t)+\sqrt{2D}\xi_1+\gamma_1(x_2-x_1),$$
$$\frac{dx_2}{dt}=-\frac{dU(x_2)}{dx_2}+I_2(t)+\sqrt{2D}\xi_2+\gamma_2(x_1-x_2), \tag{3}$$

where the white noises ξ_1 and ξ_2 of each oscillator are uncorrelated, that is, $\langle \xi_1(t)\xi_2(t')\rangle=0$. The input currents $I_1(t)$ and $I_2(t)$ are set to be identical. The coupling constants γ_1 and γ_2 can be either positive or negative; the attractive force ($\gamma>0$) and the repulsive force ($\gamma<0$) typically lead to an excitatory and an inhibitory coupling, respectively. To understand the cooperative behavior between two oscillations under couplings of different nature, in the following we consider two cases: (a) the mutual excitatory coupling $\gamma_1=\gamma_2=\gamma>0$, and (b) the mutual inhibitory coupling $\gamma_1=\gamma_2=\gamma<0$.

In Figs. 3, temporal activities of the two oscillators are shown for each case of coupling. In each figure, the firing events of the oscillators are depicted in the upper two plots. The sinusoidal graph at the bottom denotes the common periodic driving force. The long vertical line across the graphs denotes the moment when the coupling is turned on. As one can see from these figures, two oscillations are strongly synchronized for the excitatory coupling case [Fig. 3(a)], and strongly desynchronized for the inhibitory coupling case [Fig. 3(b)], as soon as the coupling is turned on. That is, the excitatory coupling typically induces synchrony between two

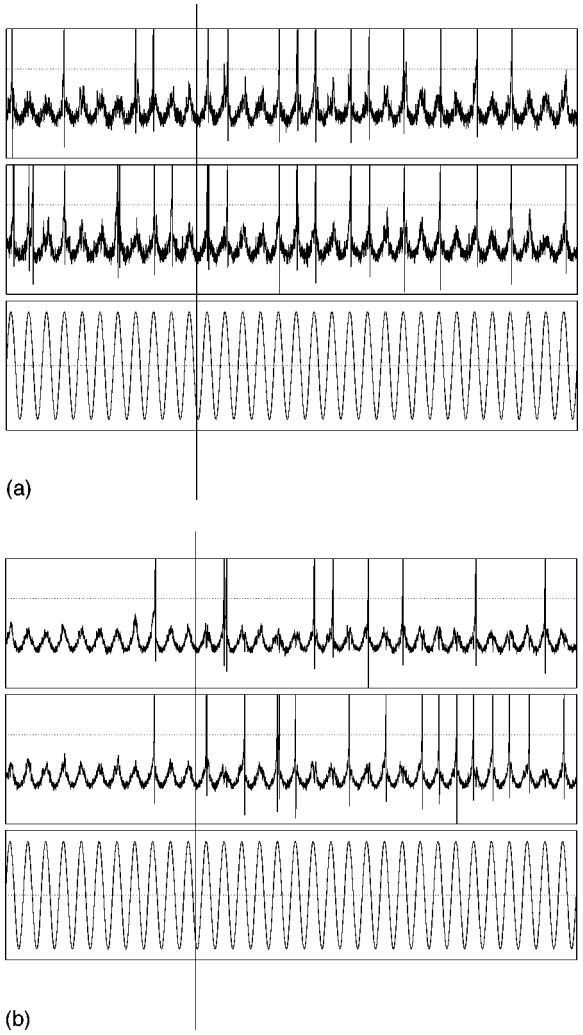

FIG. 3. Temporal activities of two coupled oscillators. The common sinusoidal forcing is depicted at the bottom of the plots. The long vertical bar across the graphs denotes the moment when the coupling is turned on. (a) The excitatory coupling ($\gamma=0.3$, $D=0.02$). (b) The inhibitory coupling case ($\gamma=-0.3$, $D=0.004$).

oscillations, whereas the inhibitory coupling induces desynchrony. One may also notice a certain amount of synchrony present even before the coupling is turned on, which is only due to the common driving force.

To see the firing response of the coupled oscillators to noise, the SNR for each coupling case has been estimated. The SNR varies depending on the coupling strength as well as the noise intensity, as shown in Fig. 4. For the excitatory coupling case, as shown in Fig. 4(a), the SNR at weaker noise intensities ($D<D_0$) is reduced, whereas it is enhanced at larger noise intensities ($D>D_0$) when compared to the single uncoupled oscillator case. This is due to the attractive force between two phases of oscillations, originating from the nature of the excitatory coupling. Enhancement of the SNR due to the excitatory coupling was previously reported for coupled oscillator systems [26,31,32].

The mechanism for the coupling dependence of the SNR can be viewed at the level of the neuronal activity as follows. The excitatory coupling tends to reduce the phase difference of the two oscillators. At a weak noise intensity, both oscillators have less chance of firings, and hence it is more likely

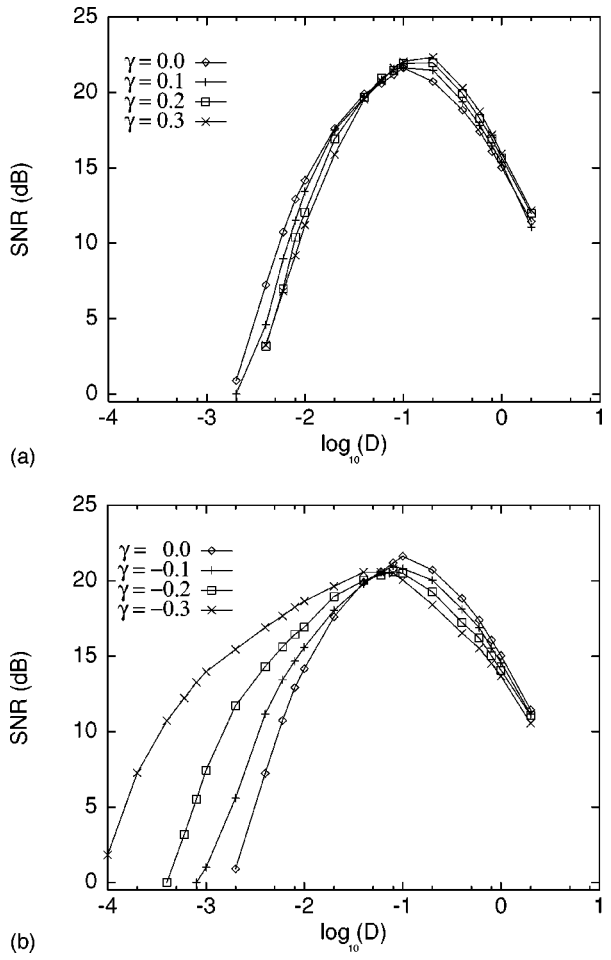

FIG. 4. SNR for two coupled oscillators with respect to the noise intensity for various magnitudes of the coupling strength: (a) the excitatory coupling and (b) the inhibitory coupling cases.

that they are in a resting state. Suppose now that the phase of one oscillator manages to get closer to the threshold and is ready to fire. The oscillator would fire only if a sufficiently strong noise kick occurs on it. However, the amount of noise should be larger than the uncoupled oscillator case, since the oscillator, now coupled, should overcome the attraction from the other oscillator at the resting state in addition to the pulling force by the nonlinear potential $U(x)$. Therefore, it is more likely that the firing of the oscillator is suppressed and, consequently, the firing rate is reduced compared to the single oscillator case. Furthermore, this effect is evidently enhanced as the coupling becomes stronger. On the other hand, when the noise intensity is large ($D>D_0$), both oscillators have more chance to be in the firing state. Even when one oscillator is in the resting state, the other oscillator in the firing state attracts the oscillator and helps firing. Consequently, the SNR will be enhanced, and this effect also becomes enhanced as the coupling is stronger.

A quite different mechanism applies to the inhibitory coupling case, since the nature of the coupling now introduces a repulsive force instead of an attractive force [see Fig. 4(b)]. It is noticeable that the change of the SNR for the inhibitory coupling case is much more prominent, especially in the weak noise regime, compared to the excitatory coupling case. This results mainly from the nature of inhibitory coupling that enhances the coupling strength effectively. That is, with excitatory coupling a small deviation of two oscillating phases tends to decrease, and the effective coupling between two oscillators becomes smaller as a result. Meanwhile, the deviation tends to increase for the inhibitory coupling case due to the repulsive force and, therefore, the effective coupling becomes larger. The increase of the effective coupling strength for the inhibitory coupling case can thus lead to a nontrivial result in the coupled oscillations, unlike for the excitatory coupling case.

Besides the noise and the driving force, the effective force between the coupled oscillations comes from the combined effect of the potential $U(x)$ and the coupling. Near the left minimum of the potential (the resting state) the potential gradient tends to synchronize the oscillations, while it tends to desynchronize the oscillations near the threshold because of the reversed curvature of the potential. Therefore, in a simplified picture, one may describe a typical firing of oscillators with inhibitory coupling by the following three steps: (1) a periodic approach of both oscillators to the threshold driven by input force, (2) a small deviation in phase due to noise, and then (3) a mutual repulsion of the phases due to the combined effect of the potential gradient and the inhibitory coupling. In step (2), the order of the phases is randomly given by noise, and the oscillator of the advanced phase will be finally led to fire by the repulsive force of step (3), whereas the other oscillator of the lagged phase is pushed back to the resting state. A more detailed analysis of the combined effect of the potential and the coupling will be given elsewhere [33].

The observation of the enhanced SNR at the weak noise intensity due to the inhibitory coupling is very important for the purpose of the segmentation performance of the oscillator network, since this implies an increased average firing rate of neurons, as will be shown in the following sections. However, since our purpose for using the coupled oscillations is their temporal activities, the desired performance of the oscillator network should also rely on the degree of phase correlations of coupled oscillators as well.

The degree of coherency between two oscillations is measured by cross correlations defined as

$$C=\frac{1}{N}\sum_{k=1}^{k=N} b_1(kT)\wedge b_2(kT),$$
$$C_A=\frac{1}{N}\sum_{k=1}^{k=N} b_1(kT)\oplus b_2(kT) \tag{4}$$

where T is the period of the input forcing, $T=2\pi/\omega_0$, and b_i is the binary representation of the activation variable; $b_i=0$ for $x<0$ and $b_i=1$ for $x>0$. $b_i(kT)$ is measured at the kth peak of the input forcing within the time window of finite width δ centered around the peak. The operations $\wedge$ and $\oplus$ denote the binary operations ''AND'' and ''Exclusive OR,'' respectively. The degree of correlation is estimated using both measures, since either measure alone does not properly estimate two kinds of correlations of interest, synchrony and desynchrony, simultaneously over a wide range of the noise intensity. The cross correlation C measures the degree of synchrony, i.e., the occurrences of synchronous firings of two oscillators at the peaks of the input forcing, while the

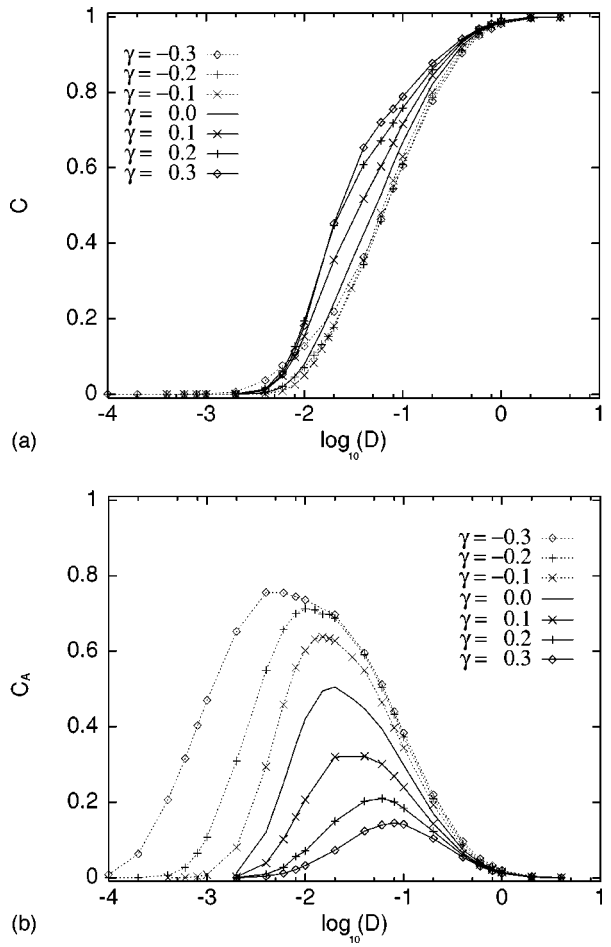

FIG. 5. Cross correlations between two coupled oscillations with respect to the noise intensity for various magnitudes of the coupling strength: (a) the cross correlation C and (b) the cross anticorrelation C_A.

anticorrelation C_A measures the degree of desynchrony. Note that two measures are independent by definition, and that the proposed definitions are different from the conventional ones. However, it is expected that these measures are more natural for the present purpose in that they measure correlations of the firing events only at the input forcing periods. As will be seen in the following sections, the desired temporal segmentation is also performed naturally at the input forcing periods in the parameter range of present interest.

Figure 5 shows that correlations between the two oscillations vary depending on the noise intensity as well as the coupling strength. When the noise intensity is sufficiently weak, the oscillators hardly fire, and hence the correlations are almost zero. As the noise intensity increases, firings start to occur and the magnitudes of both correlations rise due to the coupling between two oscillations. Note that the effect of the inhibitory coupling is more prominent compared to that of the excitatory coupling, especially in the weak noise regime. The inhibitory coupling induces strong anticorrelation at a much lower level of the noise intensity. This is, as pointed out above, due to the fact that repulsion of oscillations originating from the inhibitory coupling becomes enlarged at the weak noise level below D_0. Note also that the anticorrelation attains its maximal value at a noise intensity which is much lower compared to the peak position of the SNR curve. It is also observed that the peak shifts to a lower level of noise intensity as the coupling strength increases, which implies the important role of the inhibitory coupling at the low level of the noise intensity.

As the noise intensity becomes too strong beyond D_0, the magnitude of the cross correlations becomes small, since the firing of each oscillator is now dominated by the uncorrelated noises ξ_1 and ξ_2, and thereby the firings of the two oscillators start to be uncorrelated. In fact, this behavior at the high noise level is not reflected properly by the present definition of the cross correlation [Fig. 5(a)], which is supposed to be saturated at the higher level of noise intensity. That is, as the noise intensity increases, the oscillators tend to fire at most of the input forcing periods, and this will in turn make the cross correlation saturate even though firings in the whole time range are uncorrelated on average. However, this should not lead to confusion, since this behavior can be correctly recognized from the SNR data. Therefore, to understand more properly the cooperative behavior of the coupled oscillations, it is necessary to examine both measures of the SNR and the cross correlations.

In summary, the excitatory (inhibitory) coupling induces synchrony (desynchrony) between stochastic nonlinear oscillators. But, unlike the deterministic case, the degree of correlation depends on the noise intensity as well as on the coupling strength. Also, the firing rate of the coupled oscillator, the SNR, shows a strong dependence on both quantities. In particular, the effect of the inhibitory coupling is prominent at the lower level of noise intensity. As will be seen in the following sections, this feature of the inhibitory coupling plays an important role in accomplishing the desired temporal segmentation.

IV. STOCHASTIC OSCILLATOR NEURAL NETWORK

In Sec. III, we studied the various effects of noise and coupling on the stochastic nonlinear oscillators. In this section, using these oscillators, we construct an oscillator neural network of the Hopfield-type associative memory [8], and also examine its performance for the memory association before we proceed to apply it to the temporal segmentation tasks. The Hopfield-type neural network storing Q patterns ζ^p, $p=1\sim Q$, is described by the coupled differential equations

$$\frac{dx_i}{dt}=-\frac{dU}{dx_i}+\sqrt{2D}\xi_i+I_i(t)+\frac{\gamma}{N-1}\sum_{ij} W_{ij}(x_j-x_i), \qquad i,j=1,\ldots,N, \tag{5}$$

where N is the number of the oscillator nodes, and W_{ij} is the weight of coupling between nodes i and j. The coupling configuration is given via Hebb's rule [34],

$$W_{ij}=\sum_{p=1}^{Q}(\zeta_i^p-a^p)(\zeta_j^p-a^p), \tag{6}$$

where $a^p=\langle\zeta_i^p\rangle$, averaged over all nodes. Note that under the rule given by Eq. (6) the intragroup coupling between nodes within a group representing a same pattern is given as exci-

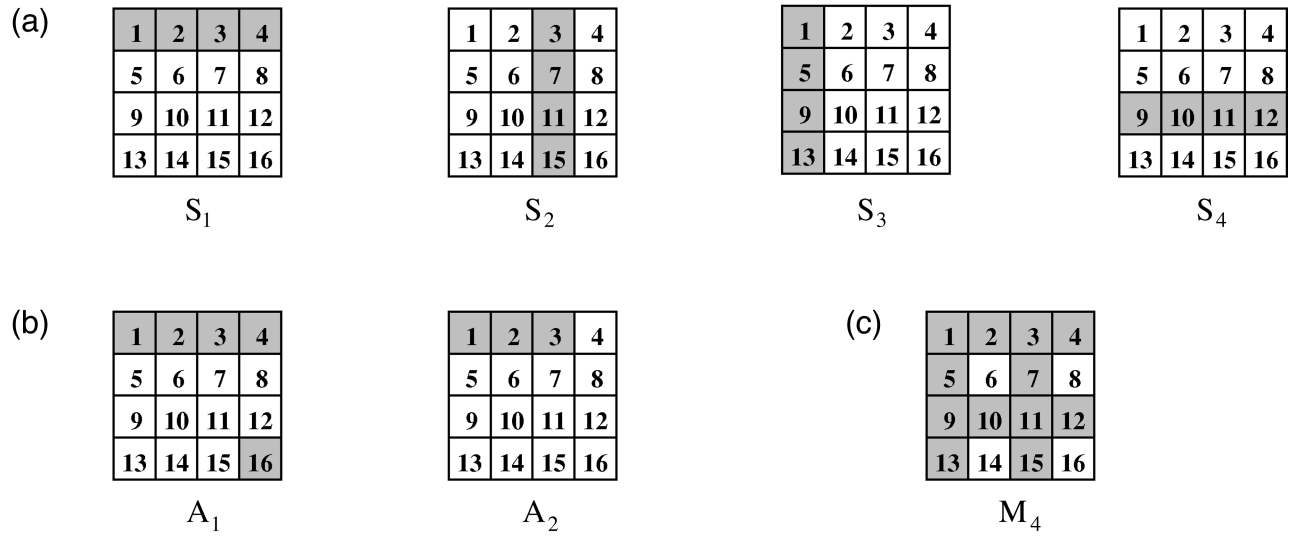

FIG. 6. (a) Stored patterns for the associative memory. (b) Test input patterns that are incomplete but close to the stored pattern S_1 with one wrong node: either an additional firing node (A_1) or a missing node (A_2). (c) Trial input pattern which is an overlapped superposition of all stored patterns. The filled box denotes the firing node and the empty box denotes the resting node.

tatory and the intergroup coupling between nodes belonging to different patterns is given as inhibitory.

For the purpose of demonstration, we consider a simple network example consisting of 4×4 oscillator nodes. Therefore, patterns ζ^p are represented by 4×4 binary data. An input pattern is given to the network by applying the subthreshold periodic force $I(t)$ to the corresponding nodes. Four patterns shown in Fig. 6(a) are stored in the memory. The filled box denotes a firing node (1), and the empty box denotes a node in the resting state (0) in the figure. Note that the nodes are labeled using numbers 1,2, . . . ,16.

To examine the association performance of the network, we use two test patterns A_1 and A_2 shown in Fig. 6(b), which coincide with the stored pattern S_1 except for one wrong node. As an associative memory we expect the network to be able to retrieve the correct pattern S_1. In the absence of coupling the oscillator nodes receiving inputs fire just in an uncorrelated fashion as depicted in Fig. 7 during the earlier time lapse. However, as the coupling is turned on at the moment denoted by a long vertical line in the figure, all four nodes belonging to S_1 fire in a synchronized fashion, which is due to both the excitatory intragroup coupling between the nodes of S_1 and the inhibitory intergroup coupling between nodes of S_1 and the others. The retrieval of S_1 is evidently successful except for some occasional failures on the excessive wrong node [Fig. 7(a)]. One may also note that retrieval is achieved within only a few periods of the driving force, so that the transient period is almost unnoticeable. The occurrence of the wrong recalls originates from the stochastic nature of the network, and the frequency of the wrong recalls varies depending both on the coupling strength and the noise intensity.

The association ratio R_{asso} measures the association performance of the network, and is defined as the averaged ratio of the number of the successful memory retrieval to the number of the input peaks. Figure 8 shows the association ratio as a function of the coupling strength for both input patterns A_1 and A_2. As can be seen from the figure, the ratio increases rapidly as the coupling strength increases. Such a tendency is expected because an increment of the coupling strength γ increases both the excitatory coupling and the inhibitory coupling between nodes. And, in turn, the increase of the excitatory coupling will enhance synchrony among nodes belonging to the same patterns, and the increased inhibition will enhance desynchrony between nodes belonging to different patterns.

From Fig. 8 one may also note that a stronger coupling is required in retrieving the stored pattern for the wrong input with missing firing nodes (A_2) than for the one with excessive firing nodes (A_1). For pattern A_1, the suppression of the excessive node $\{16\}$ is achieved mainly through the inhibitory coupling with the firing nodes $\{1,2,3,4\}$. For A_2, however, the firing of the missing node $\{4\}$ is encouraged by excitatory coupling with nodes $\{1,2,3\}$. As pointed out in Sec. III, the inhibitory coupling has a mechanism that leads to larger effective coupling. This is why the association can be carried out at a lower coupling strength for A_1, where the inhibitory coupling plays its role.

V. TEMPORAL SEGMENTATION

Now, using the STONN proposed in Sec. IV, we examine the performance of the network for the task of the temporal segmentation. That is, the segmentation into the constituent patterns is attempted for the input pattern M_4, as shown in Fig. 6(c), which is an overlapped superposition of the four stored patterns S_1–S_4.

In Fig. 9, the temporal behavior of the network is presented. The plot shows that nodes $\{1,2,3,4\}$ are selected first, and fire synchronously at the first peak time of the driving force, which leads to a successful segmentation of pattern S_1. At the next peak, pattern S_2 is now segmented. One may note, however, that the network selects and segments out the component patterns one after another in a random way as it evolves its temporal dynamics. The figure also shows that the identification of a pattern may not be always successful,

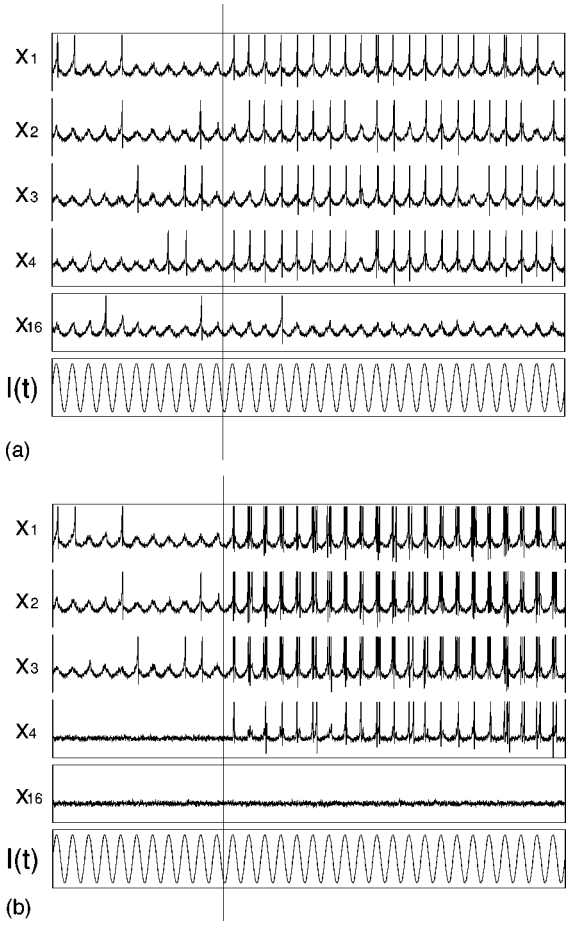

FIG. 7. Associative memory retrieval against the wrong input patterns: (a) for A_1 with one additional wrong node $\{16\}$ at $\gamma=0.9$ and $D=0.006$, and (b) for A_2 with one missing node $\{4\}$ at $\gamma=3.0$ and $D=0.006$. The long vertical line across the graphs denotes the moment when the coupling is turned on. Only the relevant nodes $\{1,2,3,4,16\}$ are shown.

as such instances are denoted by the symbol X at the bottom of the figure. For example, at the fourth peak of the forcing, nodes $\{1,2,4,5,9,13\}$ fire, which does not coincide with any stored patterns. One may regard the pattern of those firing

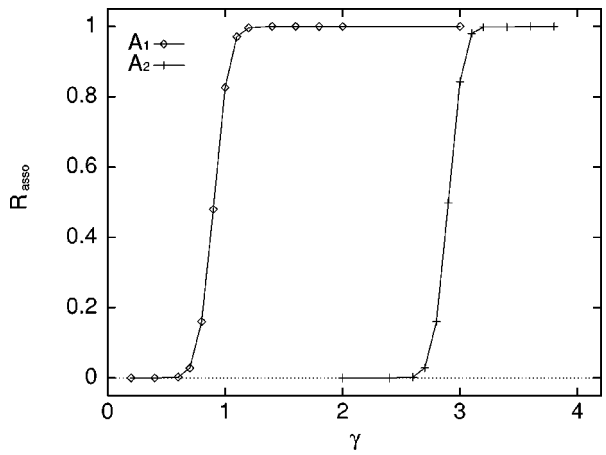

FIG. 8. Association ratio R_{asso} as a function of the coupling strength at a fixed noise intensity $D=0.006$ for the input patterns A_1 and A_2 of Fig. 6(b).

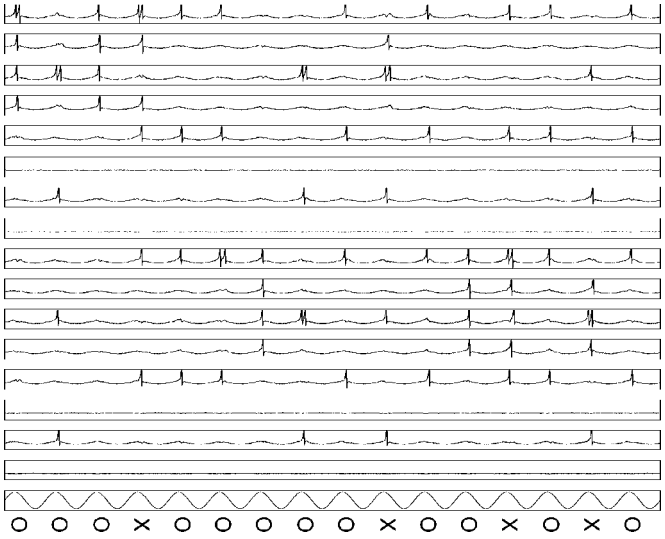

FIG. 9. Temporal segmentation of the oscillatory network for the pattern M_4 which is an overlapped superposition of all stored patterns $S_1 \sim S_4$. The parameters are chosen for the presentation purpose: $\gamma=2.0$ and $D=0.001$. The firing activities of all 16 nodes are depicted with an increasing order from the top together with the common sinusoidal forcing at the bottom. The instances of the successful segmentation are denoted by O, and the occasional failures by X at the bottom of the plot.

nodes as an incomplete segmentation of S_3 with noise at nodes $\{2,4\}$. In fact, nodes $\{2,4\}$ belong to pattern S_1, and these nodes are coupled with the nodes of S_3 via the inhibitory intergroup coupling since they belong to the different patterns. Therefore, it is likely that firing of nodes $\{2,4\}$ will be suppressed by the firing of nodes $\{1,5,9,13\}$ as the input forcing evolves. At the next peak of forcing, as one can observe from the figure, the network now selects S_3 successfully, and only nodes $\{1,5,9,13\}$ fire synchronously. However, such a decision for the next selection following an incomplete segmentation is not made in a deterministic way, again due to the random nature of the pattern selection; for example, see the segmentation failure at the tenth peak followed by S_3 selection.

The mechanism of the temporal segmentation with the random nature of the pattern selection is explained in the following. For the input pattern M_4, those neurons receiving zero input remain in the resting state. Meanwhile, the neurons receiving nonzero input signal are driven by a subthreshold periodic force, so that they are periodically driven together close to the firing threshold. Near the threshold the uncorrelated noises applied to the neurons generate small deviations in the phase of the neurons. Then a leading group of neurons of advanced phases is selected by chance and, according to the procedure explained in Sec. III for an inhibitorily coupled system, the effective repulsive force near the threshold accelerates the deviations. As the deviation grows, the coupling whose strength is proportional to the amount of the deviation becomes more effective. Then, due to the repulsive force of the mutual inhibitory intergroup coupling, the neurons of the leading group are repelled over the threshold and are able to fire. These firings of the neurons of the leading group occur synchronously due to the excitatory intragroup coupling.

Meanwhile, the lagging groups of neurons, corresponding to the other patterns, are repelled to the resting state due to the strong inhibition by the leading firing group. Therefore, desynchrony of the different patterns is achieved. Similarly, at the next peak time of the periodic forcing, another pattern among the input mixture will be selected as a leading group, and the neurons of the group will begin to fire synchronously. This explains the acting mechanism of the pattern selection and the segmentation of the proposed oscillator network in which the inhibitory coupling induces intergroup desynchrony, whereas the excitatory coupling maintains the intragroup synchrony. However, some neurons of the selected leading group may not be excited enough, and hence fail to fire in concert with other neurons of the group unless the excitatory intragroup coupling is strong enough, which leads to an incomplete segmentation of the corresponding pattern. Therefore, even though the inhibitory intergroup coupling is essential in segmenting out different patterns, the excitatory intragroup coupling is also important for a reliable performance of the network.

It is also to be noted that there exist overlappings between stored patterns. For example, node $\{1\}$ appears in both patterns S_1 and S_3. Thus this node participates both in the synchronous firings of patterns $\{1,2,3,4\}$ and $\{1,5,9,13\}$ when the network is in the course of retrieving the stored patterns S_1 and S_3 out of the input M_4. This implies that the firing rates of all neurons are not necessarily the same. That is, those neurons belonging to more than one pattern may have a higher firing rate than neurons belonging only to a single pattern.

The degree of the temporal segmentation, *the temporal segmentation ratio* R_{seg}, is measured by counting the number of instances of the complete successful segmentation and dividing it by the elapsed periods in unit T. The temporal segmentation ratio depends crucially both on the noise intensity D and the coupling strength, since these quantities influence the firing rate and the cross correlations of the coupled oscillators, as predicted from the detailed studies shown in the preceding sections. In Fig. 10, we plot the segmentation ratio as a function of the noise intensity for various magnitudes of the coupling strength. At either lower or higher noise intensities, the segmentation ratio is small since the SNR retains low values at these regimes, as implied by the two coupled oscillator cases. Optimal performance is attained at an intermediate noise intensity. Therefore, the overall appearance of the graphs resembles the SNR curve of Fig. 4.

We also note from Fig. 10 that optimal segmentation performance occurs at a much lower level of the noise intensity than $D_0 \sim 0.1$, which is the optimal noise intensity for the peak of the SNR. Optimal segmentation performance is achieved when both synchrony among the intragroup neurons and desynchrony among the intergroup neurons are strong, and also when a high level of the SNR is maintained at the same time. In fact, from the detailed behavior of the two coupled oscillators, as shown in Sec. III, we realize that the peak of the anticorrelation occurs at a much lower level of the noise intensity in the presence of the inhibitory coupling, as shown in Fig. 5(b). Furthermore, the inhibitory coupling also enhances the SNR at the weak noise intensity, as shown in Fig. 4(b). Therefore, according to the observations

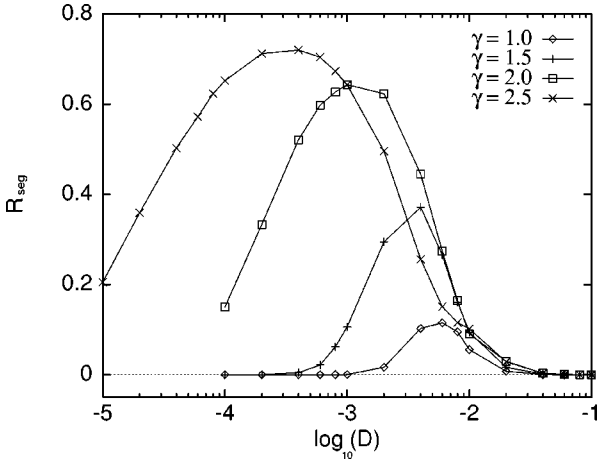

FIG. 10. Segmentation ratio R_{seg} as a function of the noise intensity for various magnitudes of the coupling strength.

from the two coupled oscillators, one may expect that the optimal performance of the network occurs at a rather low level of the noise intensity, where the inhibitory intergroup coupling establishes strong desynchrony among different patterns and also induces an enhancement of the SNR, as Fig. 10 shows. The enhanced SNR increases the cross correlation among neurons belonging to the same patterns, which leads to an enhanced intragroup synchrony as well. Similarly, the shift of the peaks to the lower level of the noise intensity can be understood from the peak shift of the anticorrelation curves, as shown in Fig. 5(b). From these observations we realize that inhibitory intergroup coupling plays a crucial role for the optimal performance of the STONN, especially in the regime of the weak noise intensity.

VI. CONCLUSIONS AND DISCUSSION

In the present work a stochastic oscillator neural network has been proposed for the task of the segmentation of superimposed patterns. Hopfield-type memory is employed by imposing an excitatory intragroup coupling between neurons belonging to the same patterns, and an inhibitory intergroup coupling between neurons belonging to different patterns. The coupling is given such that the excitatory intragroup coupling induces intragroup synchrony, whereas the inhibitory intergroup coupling induces intergroup desynchrony. That is, such temporal correlations present in the neuronal activities provide a working mechanism for the desired temporal segmentation in the proposed model.

It has been observed that the network, exploiting temporal dynamics of the coupled stochastic nonlinear oscillators, is capable of segmenting hidden constituent patterns out of an input pattern which is an overlapped superimposition of several stored patterns. The performance for the temporal segmentation, as measured by the temporal segmentation ratio, is examined in a systematic way, and is shown to vary with the noise intensity and coupling strength as well. The network, for a given coupling strength, reveals the optimal performance at an intermediate level of the noise intensity, which is reminiscent of the stochastic resonance previously observed in the coupled oscillator networks [32]. As the coupling strength increases, the performance becomes improved in general, and the level of noise intensity for the optimal

performance peak shifts to the lower value of the noise intensity. This implies that a strongly coupled network can perform the segmentation task optimally with the aid of a relatively weak noise.

We realize that the inhibitory coupling plays a crucial role in carrying out the temporal segmentation in the proposed model. As shown through detailed examinations on the two coupled oscillators in Sec. III, the inhibitory coupling enhances the SNR as well as the anticorrelation between oscillations. These are directly related to the high firing rate and the strong desynchrony among different groups of patterns for the oscillator network, both of which are essential requirements for an optimal performance of the network.

Throughout the present work we have used, as input stimuli, the subthreshold driving force and noise, which makes the segmentation mechanism quite different from previous attempts [10–12]. That is, the segmentation task is carried out in the STONN when each pattern is selected to fall into the firing state one after another by noise, while the other patterns not selected at a moment remain in the resting state; in the previous models, all pattern activities maintain oscillatory states with phase shifts among them, and such a train of the staggered oscillations is regarded as the desired segmentation. If suprathreshold stimuli are applied to the STONN, the resulting behavior would become similar to what was observed in the previous studies. That is, in this case the neurons receiving inputs are in oscillatory states, and the deterministic nature will dominate the dynamics of the coupled oscillations of the patterns, which will in turn determine the performance of the segmentation. Then, as pointed out in Ref. [14] for deterministic systems, the segmentation performance is limited within a few numbers of patterns mixed in the input, which originates from the instability of the subharmornic oscillations corresponding to the fully segmented states. Therefore, we expect that the STONN in the regime of suprathreshold stimuli will be confronted with similar limitations, as has also been observed in our simulations with the STONN. In Ref. [15], the effect of noise added to inputs for deterministic systems was also examined, and it has been observed that a noise can facilitate the performance for a slightly larger number of patterns, even though this result is not directly related to the present results since the proposed STONN utilizes the different mechanism of the temporal segmentation in the subthreshold regime. Furthermore, we also observe that the STONN in the subthreshold regime is capable of segmenting out larger numbers of superimposed patterns (up to eight), which implies that the limitation observed in the previous studies may not apply to the present approach.

Another feature of the proposed model is the periodic driving force. The role of the periodic forcing is to generate oscillations out of the one-dimensional overdamped oscillator. Consequently, it provides a natural period for the desired temporal pattern segmentation. A more important role of the periodic forcing might be that it effectively resets the phases of all firing nodes of nonzero input at each minimum of the periodic forcing, which gives the overlapped nodes more chances to fire along with the patterns which they belong to; the firing rate of the overlapped nodes should be higher for the desirable performance, as pointed out in Sec. V.

Even though there is not yet clear evidence, some implications regarding the biological relevance of the stochastic resonance have been reported, as mentioned in Sec. I, which make it plausible that the present study may provide a useful way to understand information processing in biological nervous systems. The performance of the stochastic oscillator neural network might be further improved by employing relevant perceptual processes such as selective attention [35]. It will be also interesting to identify the roles of periodic forcing and noise in the course of information processing in biological nervous systems related to the present attempts.

ACKNOWLEDGMENTS

The authors would like to thank Professor S. Kim, Dr. A. Neiman, Professor L. Schimansky-Geier, Professor F. Moss, and Dr. S. Park for useful discussions. S.K.H. was supported by the Basic Science Research Institute Program (Grant No. BSRI-96-2436), and by the CTP through the SRC Program of the Seoul National University, Korea. H.K. was supported by the Basic Science Research Institute Program (Grant No. BSRI-96-2438) of the Korean Ministry of Education.

[1] C. M. Gray, P. König, A. K. Engel, and W. Singer, Nature (London) **338**, 334 (1989).
[2] R. Eckhorn *et al.*, Biol. Cybern. **60**, 121 (1988).
[3] C. von der Malsburg and W. Schneider, Biol. Cybern. **54**, 29 (1986).
[4] H. G. Schuster, *Nonlinear Dynamics and Neuronal Networks* (VCH, New York, 1991).
[5] M. A. Arbib, *The Handbook of Brain Theory and Neural Networks* (MIT Press, Cambridge, MA, 1995).
[6] C. Koch and I. Segev, *Methods in Neuronal Modeling* (MIT, Cambridge, 1989).
[7] C. von der Malsburg, in *Brain Theory*, edited by G. Palm and A. Aertsen (Springer-Verlag, Berlin, 1986), p. 161.
[8] J. J. Hopfield, Proc. Natl. Acad. Sci. USA **79**, 2554 (1982).
[9] D. E. Rumelhart, G. E. Hinton, and R. J. Williams, Nature (London) **323**, 533 (1986).
[10] D. Horn and M. Usher, Phys. Rev. A **40**, 1036 (1989).
[11] D. Horn and M. Usher, Neural Comput. **3**, 31 (1991).
[12] D. L. Wang, J. M. Buhmann, and C. von der Malsburg, Neural Comput. **2**, 94 (1990).
[13] C. von der Malsburg and J. M. Buhmann, Biol. Cybern. **67**, 233 (1992).
[14] D. Horn and I. Opher, Neural Comput. **8**, 373 (1996).
[15] D. Horn and I. Opher, Int. J. Neural Syst. **7**, 529 (1996).
[16] K. Wiesenfeld and F. Moss, Nature (London) **373**, 33 (1995).
[17] R. Benzi, A. Sutera, and A. Vulpiani, J. Phys. A **14**, L453 (1981).
[18] B. McNamara, K. Wiesenfeld, and R. Roy, Phys. Rev. Lett. **60**, 2626 (1988).
[19] S. Fauve and F. Heslot, Phys. Lett. **97A**, 5 (1983).
[20] L. Gammaitoni *et al.*, Phys. Rev. Lett. **62**, 349 (1989).
[21] M. Dykman *et al.*, Phys. Rev. Lett. **65**, 2606 (1990).

[22] A. Longtin, A. Bulsara, and F. Moss, Phys. Rev. Lett. **67**, 656 (1991).
[23] J. K. Douglass, L. Wilkens, E. Pantazelou, and F. Moss, Nature (London) **365**, 337 (1993).
[24] I. Peterson, Science **144**, 271 (1993).
[25] E. Simonotto, M. Riani, C. Seife, M. Roberts, J. Twitty, and F. Moss, Phys. Rev. Lett. **78**, 1186 (1997).
[26] J. F. Linder, B. K. Meadows, W. L. Ditto, M. E. Inchiosa, and A. R. Bulsara, Phys. Rev. Lett. **75**, 3 (1995).
[27] A. L. Hodgkin and A. F. Huxley, J. Physiol. (London) **117**, 117 (1952).
[28] R. A. Fitzhugh, Biophys. J. **1**, 445 (1961).
[29] J. Nagumo, S. Arimoto, and S. Yoshizawa, Proc. IRE **50**, 2061 (1962).
[30] C. Morris and H. Lecar, Biophys. J. **35**, 193 (1981).
[31] A. Nieman and L. Schimansky-Geier, Phys. Lett. A **197**, 379 (1995).
[32] M. E. Inchiosa and A. R. Bulsara, Phys. Lett. A **200**, 283 (1995).
[33] S. K. Han, S. H. Park, W. S. Kim, and H. Kook (unpublished).
[34] D. O. Hebb, *The Organization of Behavior* (Wiley, New York, 1949).
[35] S. K. Han, S. W. Lee, W. S. Kim, and H. Kook (unpublished).